Thermally evaporated Cu-Al thin film coated flexible glass mirror for concentrated solar power applications

Sherine Alex[a,b,‡], Ranjith Kumar P[a,c,‡], Kamanio Chattopadhyay[a,d], Harish C. Barshilia[e,*] and Bikramjit Basu[a,c,*]

a Interdisciplinary Centre for Energy Research, Indian Institute of Science, Bangalore, India.
b Centre for Nanoscience and Engineering, Indian Institute of Science, Bangalore, India.
c Materials Research Centre, Indian Institute of Science, Bangalore, India.
d Materials Engineering, Indian Institute of Science, Bangalore, India.
e Nanomaterials Research Laboratory, Surface Engineering Division, CSIR-National Aerospace Laboratories, Bangalore 560 017, India
‡ Contributed equally

* Corresponding authors.
e-mail addresses: harish@nal.res.in (H.C. Barshilia), bikram@iisc.ac.in (B. Basu)

Thermally evaporated Cu-Al thin film coated flexible glass mirror for concentrated solar power applications

Sherine Alex[a,b,‡], Ranjith Kumar P[a,c,‡], Kamanio Chattopadhyay[a,d], Harish C. Barshilia[e,*] and Bikramjit Basu[a,c,*]

a Interdisciplinary Centre for Energy Research, Indian Institute of Science, Bangalore, India.
b Centre for Nanoscience and Engineering, Indian Institute of Science, Bangalore, India.
c Materials Research Centre, Indian Institute of Science, Bangalore, India.
d Materials Engineering, Indian Institute of Science, Bangalore, India.
e Nanomaterials Research Laboratory, Surface Engineering Division, CSIR-National Aerospace Laboratories, Bangalore 560 017, India
‡ Contributed equally

* Corresponding authors.
e-mail addresses: harish@nal.res.in (H.C. Barshilia), bikram@iisc.ac.in (B. Basu)

Abstract

This paper reports the development of mechanically flexible reflective coatings of Cu-Al intermetallic alloy on flexible glass (FG) substrates for possible concentrated solar power application. Thin films of Cu-Al intermetallic alloys were deposited on 100 μm thick FG substrates using resistive thermal evaporation of arc melted Cu-Al bulk alloy. At the optimized evaporation conditions, smooth intermetallic alloy thin films with homogeneous composition ($Cu_{0.78}Al_{0.22}$) were obtained. At a coating thickness of 160 nm, average specular and total reflectance of ~ 84% and ~ 92% respectively, were achieved. The films exhibited hydrophobic nature with a contact angle of 102°, implying the possibility of developing a self-cleaning ability. The analytical calculation involving alloy compositional dependence of plasma frequency reveals the prospect of further modulating the reflectance property by carefully tailoring thin film composition. Additionally, hard intermetallic thin film provides the opportunity of developing mirrors that may not require top protective coatings.

Keywords: Intermetallics, thin film, front surface reflectors, thermal evaporation.

1. Introduction

Concentrated solar power (CSP) system represents a major emerging technology for the conversion of solar energy to electricity[1, 2]. The increasingly widespread applications of solar thermal technologies demand development of advanced solar reflector materials with excellent optical properties and long-term durability[3]. Two separate wavelength intervals[4] are distinguished for solar energy research. The primary and fundamental one is the visible solar spectrum (280 - 2500 nm), which contains the energy we wish to exploit. The second one is the thermal infrared spectrum (> 2500 nm). Specular reflectance refers to that part of the incident beam that gets reflected at the same angle as the angle of incidence. The solar-weighted specular reflectance of a solar mirror[5] is estimated using the values of the measured specular reflectance spectrum and the direct solar irradiance spectrum at different wavelength intervals. Maintaining minimum angle of acceptance provides lesser diffused light and a constant angle of incidence throughout the surface that enables enhanced focussing of the light rays onto the receiver. A high reflectance in the entire wavelength range of the solar spectrum (280 - 2500 nm) is a crucial optical requirement for reflectors in solar thermal applications.

Flexible glass (FG) substrates[6, 7] used in this investigation are of 100 μm thick and these light-weight FG has significant advantages over conventional mirrors for applications in CSP technology. It also exhibits superior anti-permeation properties against oxygen and moisture[8], while at the same time ensuring sufficient mechanical flexibility and low-cost roll-to-roll fabrication processes. Although front surface mirrors have been developed to be bendable and lightweight, their optical performance severely degrade in only a couple of months, if the surface is not protected[9, 10].

The motivation for the present study on the Cu-Al system stems from our earlier work. In a recent publication, we have shown that Cu-Al intermetallic alloys[11],

corresponding to the intermetallic $Cu_{0.78}Al_{0.22}$ and Cu_3Al phase, possess high specular reflectance of > 89% together with good mechanical properties and hydrophobicity. We postulate that this alloy, if successfully coated on a flexible substrate, can lead to the development of scratch resistant solar mirror for dusty and environmentally harsh locations.

In this paper, a facile preparation of highly reflective and adhesive Cu-Al films by resistive thermal evaporation of the Cu-Al arc melted ingots is reported. We further analyze the phase compositions, surface morphology, thickness and surface coverage of this novel coating on FG and evaluate its optical and mechanical properties for CSP applications.

2. Experimental and Instrumentation

2.1. Materials and Methods

Pre-cut (25 mm x 25 mm) Corning® Willow® Glass substrates (thickness 100 μm) received from Corning were used for the present work. Prior to deposition, the substrates were ultrasonically cleaned with isopropanol and then washed with deionized water several times. The substrates were then soaked in a cleaning solution (labolene) and further sonicated for 15 min. Finally, the substrates were cleaned with deionized water and placed in a cleaned container after drying for experimental use.

Elemental shots of copper and aluminium (purity 99.99%, Alfa Aesar) were used for preparing a Cu-21.2 atomic % Al alloy by arc melting. The homogenisation was ensured by melting the ingot multiple times. These Cu-Al ingots were precut into smaller pieces (10 mm x 2 mm x 1 mm) and were used as target material for resistive thermal evaporation deposition under a vacuum of ~ 0.5 mPa. The source to substrate distance was kept approximately 30 cm. The vaporised alloy was allowed to naturally deposit onto the FG substrate to form a uniform layer. The depositions were carried out at a rate of 0.5 $Å s^{-1}$. The coating deposition rate is one of the key parameters that determine the nature of the film[12]. When deposition rate was lower than 0.5 $Å s^{-1}$, a non-homogeneous coating was obtained. At a higher

deposition rate, films with high surface roughness were obtained. The deposition rate was initially optimized by changing the value of the electric current supplied to the tungsten wire basket containing the source material. At an optimized deposition rate of 0.5 $Å s^{-1}$, single-phase $Cu_{0.78}Al_{0.22}$ alloy was obtained. All subsequent experiments were carried out with this deposition rate.

2.2. Characterization

For structural characterisation, X-ray diffraction (XRD) patterns were obtained using a computer controlled RIGAKU, X-ray diffractometer using $CuK\alpha$ radiation. The scanning angle was varied from 10 to 90^o in a step of 0.24^o /sec. The composition of the intermetallic coatings was characterized using electron probe microanalyzer (EPMA) (JEOL-JXA 8530 field emission electron probe microanalyzer, Japan). The surface morphology of the Cu-Al coating was studied using atomic force microscope (AFM) (Nanosurf easy scan 2, Nanosurf Inc., USA).

The chemical composition and surface oxidation of the Cu-Al bulk material were determined using X-ray photoelectron spectroscopy (XPS) (SPECS) with non-monochromatic Al Kα radiation (1486.8 eV). The binding energies were internally calibrated with reference to the adventituous component of the C1s peak, fixed at 284.7 eV (Figure 10(d)). The thickness of the coating was measured using non-contact optical profilometer (CCI MP TalySurf, Ametak, UK) and Dektak profilometer (Dektak XT Stylus Profiler, USA). Specular reflectance was measured at 8^o incident angle and 20 nm slit width using UV-Visible-NIR integrating sphere spectrophotometer (Perkin Elmer Lambda 950 with Universal Reflectance Accessory attachment, USA). Before measuring, the instrument was calibrated by measuring the reflectance of NIST standard sample (# SRS - 99 - 020 AS - 011 610 - 060). The reflectance of this sample was in between 98.5 - 99.2% in the wavelength region of 400 – 1600 nm. The contact angle measurements were performed using contact

angle goniometer OCA 15EC (Video based contact angle measuring unit with software SCA 20, DataPhysics Instruments, Germany). For scratch adhesion, a 200 μm tip radius Rockwell diamond indenter is moved over the specimen surface of 2 mm at a speed of 0.02 mm/s, with a linearly increasing load from 300 mN to 1 N.

3. Results and Discussion

3.1. Phase assemblage by XRD

The X-ray diffraction pattern in Figure 1(a) shows the presence of two different intermetallics, Cu_3Al (β_1 phase) (JCPDS card No: 00-028-0005) and $Cu_{0.78}Al_{0.22}$ compound (JCPDS card No: 04-006-6355) in the as-cast alloy. Representative scanning electron microscopy image of Cu-Al alloys is shown in Figure 1(b). The microstructure of Cu-21.2 atomic % Al reveals a eutectoidal reaction. A modest hardness of 2.1 GPa was measured using a well-polished surface that also exhibit an average specular and solar reflectance[13], calculated by weighting with ASTM G173 solar spectra for AM 1.5, of 89.5 % and 83 % respectively (see Figure 1(c)).

Figure 2 shows the nature of the as-deposited lustrous reflective film. The homogeneous nature of the deposited film can be seen in Figure 2(a). In order to check the clarity of reflection, the camera was only focussed on the reflection, rather than both the mirror and reflection. The clarity of the reflected image of the tower building on the deposited film as revealed in Figure 2(b), establishes its efficacy as a good optical reflector. The phase analysis of the as-deposited film, performed by glancing angle XRD is indicated in Figure 3. There is a broad peak from the glass substrate when the thickness of the film is very small. However, with increasing thickness and coverage this peak disappears. All the other X-ray reflections obtained from thin films of varying thicknesses can be indexed in terms of a cubic structure, corresponding to $Cu_{0.78}Al_{0.22}$ intermetallic compound. No amorphous phase from the evaporated layer could be observed, indicating that the nucleation rate of the

crystalline intermetallic phase on the substrate is very high. The first three reflections appearing in the patterns have interplanar spacings of 2.199 Å (2θ = 42.6°), 1.835 Å (2θ = 49.6°) and 1.298 Å (2θ = 72.8°) respectively that can be indexed as the planes (111), (200) and (220) of a cubic lattice respectively. We note that the peak positions of the reflections do not vary with thickness, indicating the consistency in coating composition during deposition. The lattice parameter of the $Cu_{0.78}Al_{0.22}$ compound was estimated to be ~ 3.639 Å, while the crystallite size was found to be ~ 44 nm. We have also observed appreciable increase in intensity of (220) peak for a coating thickness of 160 nm. This observation can perhaps be attributed to the strain energy minimization during grain growth along (220) plane and this corroborates well with previous literature reports indicating critical thickness window[14]. Texture analysis was quantitatively carried out using Harris method[15]. The texture coefficient (TC_{hkl}) of each crystallographic plane (hkl) and the degree of orientation (σ) were calculated using the following relations[15, 16]

$$TC_{hkl} = \frac{{I_{hkl}}/{I^0_{hkl}}}{({1}/{N})\sum_{N=1}^{N} {I_{hkl}}/{I^0_{hkl}}} \quad (1)$$

$$\sigma = \frac{\sqrt{\sum_{N=1}^{N}(TC_{hkl}-1)^2}}{\sqrt{N}} \quad (2)$$

where, I_{hkl} is the integrated intensity of (hkl) peak obtained from diffraction pattern of the sample, I^0_{hkl} is the standard integrated intensity from the reference JCPDS file, N is the number of diffraction planes. In the present case, only (111), (200) and (220) are considered and therefore, N = 3.

3.2. Coating surface characteristics

The compositional homogeneity of the film was determined by performing line scan using wavelength dispersive spectroscopy (WDS) detector in EPMA, having crystals of copper and aluminum. A uniform composition of ~ 78 atomic % Cu and ~ 22 atomic % Al

was recorded (Figure 5a). Compositional mapping confirms the homogeneity of the film, shown in Figure 5(b-c), where the average composition of the film was measured to be ~ 80.7 atomic % Cu and ~ 19.3 atomic % Al with an instrumental error + 1 %. The thickness of the as-deposited coating was measured using optical profilometer (Figure 6a) and Dektak profilometer (Figure 6b). The summary of thickness measurements performed using both the techniques is given in Table 1. A critical look at Table 1 reveals that both the measurement techniques provide comparable thickness with a difference of 1 - 2 nm for nominal coating thickness of less than 100 nm. Above 100 nm, the difference in two different measurement techniques can be 3 - 4 nm.

To gain more knowledge on film morphology, contact mode AFM was used to study the morphology and surface roughness of the Cu-Al film. The reflectance properties critically depend on the roughness of the surface. Specular reflectance is realised for a smooth surface, i.e., when the surface irregularities are comparable to the wavelength of the incident light. When the surface roughness is higher than the wavelength of the incident light, diffuse reflectance takes place[17]. The roughness parameters, arithmetic average (R_a) of absolute values and root mean squared (R_q) values measured over a 50 μm square of the Cu-Al coating were found to be < 10 nm. The R_a of the FG measured over the same above area was 7 nm. R_a is the average surface roughness of the measure 2D profile of the given sample length. Whereas, R_q is the standard deviation of the height distribution for the sampling length. Any small variation in the profile gives a large deviation in the R_q value. Two surfaces with identical R_a values can have different R_q values[18]. Different R_q values can lead to different reflectivity. Hence, we have mentioned both the values to distinguish any measurable differences of the surface roughness. The R_a and R_q values of the films, shown in Table 1, confirm that the film surface has the desired roughness for reflector application. The surface roughness of the film can be increased by increasing the rate of deposition, but it decreases

the specular reflectance for the same thickness of Cu-Al film. During resistive thermal evaporation, the rate of deposition was optimized to be 0.5 $Å s^{-1}$, where the average roughness was found to be less than 10 nm.

3.3. Optical reflectance

The specular and total reflectance of the Cu-Al films of different thickness were measured using light of wavelength ranging from 280 - 2500 nm. The specular reflectance spectra of the Cu-Al film with varying thickness on flex glass are shown in Figure 7(a). 40 nm thick Cu-Al film exhibited average specular reflectance value of ~ 70%. The film with 160 nm thickness exhibited average specular reflectance of ~ 84%. The solar reflectance was calculated by weighting with ASTM G173 solar spectra for AM 1.5. The solar weighted specular reflectance[13], for 160 nm film was calculated to be ~ 73.5%. The variation of total reflectance with thickness of the Cu-Al film on flex glass substrate is shown in Figure 7(b). The average total reflectance of ~ 92% was recorded with 160 nm Cu-Al film.

The variation of specular reflectance and total reflectance with coating thickness is presented in Figure 7(c). The specular reflectance and total reflectance of the Cu-Al films are higher than the substrate and exhibited almost a direct relationship with increasing film thickness of up to 160 nm. The average specular reflectance and average total reflectance are found to reach almost steady state values of 84% and 92%, respectively, at a coating thickness of 160 nm.

To compare, the specular reflectance of films with increasing thickness on soda lime glass is also presented in Figure 7(d). The film with 160 nm thickness exhibited maximum average specular reflectance of ~ 83%. Thus, irrespective of substrates, similar behaviour of maximum reflectance at 160 nm thickness was recorded in all the above cases. The summary of various reflectance measurements performed using Cu-Al film is provided in Table 1.

3.4. Wettability and scratch resistance

We have also evaluated the wetting behaviour of the surface by sessile water droplet technique. The water droplet contact angle on the flex glass substrate is 29.2 + 2.3° (Figure 8(a)), indicating a strong hydrophilic nature. Figure 8(b-e) indicates the morphology of water droplet on the thermally evaporated Cu-Al coating with varying thicknesses from 40 to 160 nm, respectively. The 160 nm Cu-Al film exhibited a contact angle of 102.1 + 0.7°, indicating the hydrophobic nature of the film. The contact angles measured in all the films were found to be above 97° that indicate the hydrophobic capability for the coatings (see Table 1).

To determine the scratch resistance and the film adhesion, scratch adhesion test was performed on the coatings by applying a linearly increasing load from 300 mN to 1 N. Each scratch was examined with the help of an optical microscope for determining the crack initiation point. Initially, the film is tested for a load up to 900 mN, where no visible crack can be seen along the entire length of the scratch (Figure 9(a)). However, on increasing the load to 1 N, crack is visible (Figure 9(b)), indicating that the film is unstable after 900 mN. This observation confirms that the coating can withstand a load of 900 mN or below.

3.5. Discussion

We first probe the origin of modest specular reflectance property of bulk Cu-Al intermetallics. The XPS analysis of bulk Cu-Al intermetallics was carried out. The peaks at 932.25 and 952.08 eV in Figure 10(a) shows the splitting of copper into two sublevels $2p_{1/2}$ and $2p_{3/2}$, respectively. The peak at 932.25 eV shows that there is a shift in the electron cloud towards copper from aluminium since the electronegativity of copper is higher than that of aluminium. Hence, we can safely conclude that the copper is bound to aluminium and not to oxygen[19]. Also, the absence of satellite peaks indicates that the oxides of copper is not formed during thermal evaporation[20-22]. The deconvoluted Al 2p peaks at 74.80 and 77.18 eV in Figure 10(b) represent the presence of Al_2O_3 and crystalline anhydrous γ-Al_2O_3 phases,

respectively. This Also, the absence of Al peak proves the fact that an oxide layer is formed on the surface. The deconvoluted O 1s peaks at 530.69 and 532.30 eV support the formation of aluminium oxides and chemisorbed oxygen (see Figure 10(c))[23, 24]. It has been reported that aluminium exhibits very high reflectance in the UV-visible regions. In particular, the spectral reflectance for aluminium is in the range of 80 - 85% in the UV region. Whereas, copper exhibited spectral reflectance of 20 - 30% in the UV region[25, 26]. In the case of Cu-Al intermetallics used in the present work, the aluminium content is ~ 22 atomic %. Therefore, the reflectance data presented in Figure 1 and Figure 7, indicates the intrinsic behaviour of Cu-Al intermetallic reflectance. As compared to the bulk material, the reflectance of the thin film shows a minor change at the lower wavelength region of the spectrum due to the presence of oxides, as confirmed by XPS. Results of our experiment do not show any crystalline peaks of Al_2O_3 in the XRD pattern, indicating the amorphous nature[27]. Formation of such amorphous oxides under metastable conditions is reported in the literature[28]. The selective oxidation behaviour in Cu-Al alloys is due to Al having greater oxygen affinity than Cu[29, 30]. This layer of Al_2O_3 will act as a protective barrier and inhibit further oxidation.

As published in our previous article[31], the Cu-Sn alloy, when exposed to 90% relative humidity at 50 °C for 3 days, exhibited only 8.5% drop in specular reflectance. Similar coatings were also subjected to weather testing by placing them next to roof top solar cells at parallel and 14.5° orientation. The dust accumulation on pure Al film was around 30% more than that on Cu-Sn film at 14.5° orientation. All these observations support good humidity and weather resistance of Cu-alloy thin film. In line with such observations together with the fact that the oxides of aluminium exhibit excellent corrosion resistance[32, 33], it is expected that Cu-Al thin film coating will have desired degradation resistance. The advantage that Cu-Al thin film has over the commercially available mirrors is that it does not require

any additional techniques to deposit a protective top layer coating. A transparent thin film of oxide layer of specific thickness and refractive index has anti-reflection property which will affect the reflecting properties[34]. Thus, even though some reflectance (~ 1%) will be lost due to the presence of the amorphous oxide layer, the film does not exhibit any drastic antireflection behaviour.

In general, the reflectance of a surface is enhanced by a thin film of high refractive index. The refractive index and coating thickness play an important role in defining the reflectance from the coated surface. If the coating thickness is too low then the film will partially reflect and partially transmit (assuming that it is non-absorbing in nature). On the other hand, when the coating thickness is too high, then the surface roughness also plays an important role, which decreases the reflection because of diffused reflection. This indicates the existence of the critical thickness range for better reflectance of thermally evaporated coatings.

The refractive index depends on the composition and density of the film as well as the surface oxidation. The density of thin film is expected to be less than that of bulk material of similar composition, because of the presence of pin holes and porosity in the film. In a polycrystalline film, the microstrain, generated during film deposition and grain growth, determines the porosity and the density. The surface, interface and strain energy minimisation determine the grain growth and texture evolution in a polycrystalline film. Also, the substrate has different thermal and elastic properties. This causes abnormal grain growth and strain in the film. For the same deposition conditions, the strain energy minimisation dominates the surface and interface energy minimisation at a particular thickness window. This causes abnormal growth along (110) orientation in a polycrystalline film[35]. Figure 3 shows that at a thickness of 160 nm, there is preferred orientation along (220) direction. The TC_{hkl} of each peak is calculated according to Harris method and the results are presented in Figure 4. The

calculation of TC reveals that there is a preferred orientation along (220) direction, albeit the degree of preferred orientation remains constant (σ = 3) at different thicknesses. This supports the observations made from XRD results. From Figure 4, we observe that, at an initial coating thickness of 40 nm, the growth along (111) direction dominates. As the thickness of the film increases, the growth along (200) plane is depleted and becomes relatively very low at the thickness of 160 nm. Also, we can observe the growth contention between the (111) and (220) planes as the thickness is increased. At the thickness of 160 nm, the growth along (220) direction prevails over the growth along the other two directions. This can be attributed to the strain energy minimisation[14, 16] and hence the relatively higher reflectance of coating of 160 nm thickness was obtained than that at other thicknesses. Therefore, it can be stated that the reflectance of the Cu-Al thin film is influenced by the thickness and texture.

We shall now discuss the role of film composition on the specular reflectance properties. Plasma edge is one of the most prominent optical phenomena in solids, the point at which free electrons in the material start vibrating collectively[36]. For photon of wavelength less than that associated with the onset of this oscillation, there will be a steep drop in reflectance, which in turn is determined by the plasma frequency of the material. The variations in reflectance in different materials are associated with the plasma edge of the material. The spectral location of the plasma edge is determined by the free electron density. The electric and magnetic fields in a metal created due to the electrons and lattice are in equilibrium. But when an electromagnetic radiation (e.g. solar radiation) is incident on the metal surface, this equilibrium is disturbed and an oscillation due to Coulombic force that tries to restore the equilibrium position of the electrons is produced. The frequency at which these oscillations resonate is called the "plasma frequency" (ω_p), which plays a crucial role in the propagation of electromagnetic waves. The plasma frequency is determined by the

electron density and can be calculated if the material density and molecular mass are known. The plasma frequency of a non-plasma material is due to the natural collective oscillation frequency of the sea of electrons in the material and is given by,

$$\omega_p = \sqrt{\frac{ne^2}{m\epsilon_o}} \quad (3)$$

where, n is the free electron density, e is the elementary charge (1.602 x 10^{-19} C), m is the electron mass (9.1 x 10^{-31} Kg) and ϵ_o is the permittivity of free space (8.854 x 10^{-12} Fm^{-1}).

Higher the free electron density, the higher will be the plasma frequency. The free electron density (n) can be obtained by multiplying number of atoms per unit volume (N_v) and electrons per atom (e/a).

$$n = N_v \times (e/a) \quad (4)$$

The electron concentration (e/a) for an intermetallic compound A_aB_b is determined using Hume Rothery rule[37, 38], $(e/a) = \frac{ax + by}{a+b}$ (5)

where, x and y are the respective group numbers of elements A and B in the old periodic table and a and b are the number of atoms in the molecular formula, respectively.

Further, the number of atoms per unit volume (N_v) can be determined as,

$$N_v = (N_A \times \rho)/M \quad (6)$$

where, N_A is the Avogadro number (6.022 x 10^{23}), ρ is the density and M is the atomic mass.

Substituting equation (2), (3) and (4) in (1), we get the expression for plasma frequency as,

$$\omega_p = \sqrt{\frac{(N_A \times \rho) \times (ax+by)\, e^2}{Mm\epsilon_o\, (a+b)}} \quad (7)$$

From equation (5), it is evident that the plasma frequency is directly proportional to the square root of the ratio of the density to its molecular weight of the material and also to the square root of electron concentration. Thus, a material having higher electron concentration and higher density together with lower molecular weight, can be preferred as a

reflector material. In a demonstration of this rational, we have earlier shown the role of plasma frequency in determining the reflector properties of intermetallic alloys[11]. The substitution of Al in Cu-Sn alloy shifts the plasma edge towards the UV region, which increases the reflectance property.

The electron density of $Cu_{0.78}Al_{0.22}$ phase was found to be ~ 116.55 x 10^{27} per m^3 and the plasma frequency was calculated to be ~ 19.25 x 10^{15} rad/s. This frequency lies near the UV region (~ 10^{16} rad/s) of the solar spectrum. Thus, it can be hypothesized that the presence of pure $Cu_{0.78}Al_{0.22}$ phase in a thin film with desired thickness (minimum transmission) can improve the reflectance, as per plasma frequency calculation.

4. Conclusions

In summary, Cu-Al thin film intermetallic alloys were deposited on 100 μm thick flexible glass substrates by resistive thermal evaporation. The presence of single phase $Cu_{0.78}Al_{0.22}$ in the film was confirmed by XRD analysis. At a thickness of 160 nm, the film exhibited high reflectance and preferred orientation growth along (220) direction due to strain energy minimization. Qualitatively, similar thickness dependency of specular reflectance was achieved, independent of substrate (flexible glass or soda lime glass). The average specular and total reflectance of 160 nm Cu-Al coating of flexible glass were measured to be 83.9% and 92.1%, respectively. An attempt has been made to correlate the reflectance with the plasma edge and preferential crystallographic growth of coatings. The film exhibited hydrophobic nature and good coating adhesion was confirmed from the scratch resistance at 900 mN load.

Acknowledgements

This work is supported in part under the US-India Partnership to Advance Clean Energy-Research (PACE-R) for the Solar Energy Research Institute for India and the United States (SERIIUS), funded jointly by the U.S. Department of Energy (Office of Science, Office of

Basic Energy Sciences, and Energy Efficiency and Renewable Energy, Solar Energy Technology Program, under Subcontract DE-AC36-08GO28308 to the National Renewable Energy Laboratory, Golden, Colorado) and the Government of India, through the Department of Science and Technology under Subcontract IUSSTF/JCERDC-SERIIUS/2012 dated 22nd Nov. 2012. The authors also appreciate the help rendered by Mr Srinivas Govindappa, NAL, Bangalore for the measurements of specular reflectance and Scratch test. Sherine Alex is thankful to Dr Arvind Kumar, NAL, Bangalore for helping in performing thermal evaporation work.

References

[1] D. Barlev, R. Vidu, P. Stroeve, Innovation in concentrated solar power, Solar Energy Materials and Solar Cells, 95 (2011) 2703-2725.
[2] R. Enger, H. Weichel, Solar electric generating system resource requirements, Solar Energy, 23 (1979) 255-261.
[3] C. Kennedy, K. Terwilliger, Optical durability of candidate solar reflectors, ASME 2004 International Solar Energy Conference, American Society of Mechanical Engineers, 2004, pp. 597-606.
[4] A. Roos, Use of an integrating sphere in solar energy research, Solar Energy Materials and Solar Cells, 30 (1993) 77-94.
[5] Aránzazu Fernández-García, Florian Sutter, M. Montecchi, Fabienne Sallaberry, Anna Heimsath, Carlos Heras, Estelle Le Baron, A. Soum-Glaude, Parameters and method to evaluate the reflectance properties of reflector materials for concentrating solar power technology, SolarPACES Guideline version 2.5, (March 2018) 1-33.
[6] M.M. Tavakoli, K.-H. Tsui, Q. Zhang, J. He, Y. Yao, D. Li, Z. Fan, Highly efficient flexible perovskite solar cells with antireflection and self-cleaning nanostructures, ACS nano, 9 (2015) 10287-10295.
[7] W. Rance, J. Burst, D. Meysing, C. Wolden, M. Reese, T. Gessert, W. Metzger, S. Garner, P. Cimo, T. Barnes, 14%-efficient flexible CdTe solar cells on ultra-thin glass substrates, Applied Physics Letters, 104 (2014) 143903.
[8] H. Mahabaduge, W. Rance, J. Burst, M. Reese, D. Meysing, C. Wolden, J. Li, J. Beach, T. Gessert, W. Metzger, High-efficiency, flexible CdTe solar cells on ultra-thin glass substrates, Applied Physics Letters, 106 (2015) 133501.
[9] A. Czanderna, Stability of interfaces in solar energy materials, Solar Energy Materials, 5 (1981) 349-377.
[10] A. Roos, C.G. Ribbing, B. Karlsson, Stainless steel solar mirrors—a material feasibility study, Solar energy materials, 18 (1989) 233-240.
[11] S. Alex, K. Chattopadhyay, B. Basu, Tailored specular reflectance properties of bulk Cu based novel intermetallic alloys, Solar Energy Materials and Solar Cells, 149 (2016) 66-74.
[12] K. Bordo, H.-G. Rubahn, Effect of deposition rate on structure and surface morphology of thin evaporated Al films on dielectrics and semiconductors, Materials Science, 18 (2012) 313-317.

[13] G. Committee, Tables for reference solar spectral irradiances: Direct normal and hemispherical on 37 tilted surface, ASTM International, (2012).
[14] C.V. Thompson, R. Carel, Texture development in polycrystalline thin films, Materials Science and Engineering: B, 32 (1995) 211-219.
[15] V. Consonni, G. Rey, H. Roussel, D. Bellet, Thickness effects on the texture development of fluorine-doped SnO_2 thin films: The role of surface and strain energy, Journal of Applied Physics, 111 (2012) 033523.
[16] X. Sun, K. Gao, X. Pang, H. Yang, Interface and strain energy revolution texture map to predict structure and optical properties of sputtered PbSe thin films, ACS applied materials & interfaces, 8 (2015) 625-633.
[17] H. Bennett, J. Porteus, Relation between surface roughness and specular reflectance at normal incidence, JOSA, 51 (1961) 123-129.
[18] B. Basu, M. Kalin, Surfaces and Contacts, Tribology of ceramics and composites: a materials science perspective, John Wiley & Sons, (2011), pp. 39-41.
[19] Y. Shi, Y. Zhou, D.-R. Yang, W.-X. Xu, C. Wang, F.-B. Wang, J.-J. Xu, X.-H. Xia, H.-Y. Chen, Energy level engineering of MoS_2 by transition-metal doping for accelerating hydrogen evolution reaction, Journal of the American Chemical Society, 139 (2017) 15479-15485.
[20] M. Al-Kuhaili, Characterization of copper oxide thin films deposited by the thermal evaporation of cuprous oxide (Cu_2O), Vacuum, 82 (2008) 623-629.
[21] C.-K. Wu, M. Yin, S. O'Brien, J.T. Koberstein, Quantitative analysis of copper oxide nanoparticle composition and structure by X-ray photoelectron spectroscopy, Chemistry of materials, 18 (2006) 6054-6058.
[22] S. Poulston, P. Parlett, P. Stone, M. Bowker, Surface oxidation and reduction of CuO and Cu_2O studied using XPS and XAES, Surface and Interface Analysis, 24 (1996) 811-820.
[23] B. Schnyder, R. Kötz, Spectroscopic ellipsometry and XPS studies of anodic aluminum oxide formation in sulfuric acid, Journal of Electroanalytical Chemistry, 339 (1992) 167-185.
[24] N. Reddy, P. Bera, V.R. Reddy, N. Sridhara, A. Dey, C. Anandan, A.K. Sharma, XPS study of sputtered alumina thin films, Ceramics International, 40 (2014) 11099-11107.
[25] E.W. Spisz, A.J. Weigand, R.L. Bowman, J.R. Jack, Solar absorptances and spectral reflectances of 12 metals for temperatures ranging from 300 to 500K, National Aeronautics and Space Administration, Cleveland, Ohio (USA). Lewis Research Center, 1969.
[26] W.M. Rohsenow, H.Y. Choi, Heat, mass, and momentum transfer, Prentice hall, New Jersey, (1961).
[27] P. Nayar, A. Khanna, D. Kabiraj, S. Abhilash, B.D. Beake, Y. Losset, B. Chen, Structural, optical and mechanical properties of amorphous and crystalline alumina thin films, Thin Solid Films, 568 (2014) 19-24.
[28] E.J. Lavernia, J. Ayers, T.S. Srivatsan, Rapid solidification processing with specific application to aluminium alloys, International materials reviews, 37 (1992) 1-44.
[29] M. Sanderson, J. Scully, The selective oxidation behaviour of some Cu Alloys, Corrosion Science, 10 (1970) 165-173.
[30] G. Plascencia, T.A. Utigard, High temperature oxidation mechanism of dilute copper aluminium alloys, Corrosion Science, 47 (2005) 1149-1163.
[31] S. Alex, B. Basu, S. Sengupta, U.K. Pandey, K. Chattopadhyay, Electrodeposition of δ-phase based Cu–Sn mirror alloy from sulfate-aqueous electrolyte for solar reflector application, Applied Thermal Engineering, 109 (2016) 1003-1010.
[32] M. Fedel, C. Zanella, S. Rossi, F. Deflorian, Corrosion protection of silver coated reflectors by atomic layer deposited Al_2O_3, Solar Energy, 101 (2014) 167-175.
[33] Y. Yang, A. Kushima, W. Han, H. Xin, J. Li, Liquid-like, self-healing aluminum oxide during deformation at room temperature, Nano letters, 18 (2018) 2492-2497.

[34] M. Keshavarz Hedayati, M. Elbahri, Antireflective coatings: Conventional stacking layers and ultrathin plasmonic metasurfaces, a mini-review, Materials, 9 (2016) 497.
[35] C. Thompson, R. Carel, Grain growth and texture evolution in thin films, Materials Science Forum, Trans Tech Publ, 1996, pp. 83-98.
[36] A.E. Dixon, J.D. Leslie, Solar energy conversion: an introductory course, Elsevier, 2013.
[37] W. Hume-Rothery, R.E. Smallman, C.W. Haworth, The structure of metals and alloys, The Institute of Metals, 1 Carlton House Terrace, London SW 1 Y 5 DB, UK., (1988).
[38] U. Mizutani, The Hume-Rothery rules for structurally complex alloy phases, in: E. Belin-Ferré (Ed.) Surface Properties And Engineering Of Complex Intermetallics, World Scientific, (2010), pp. 323-399.

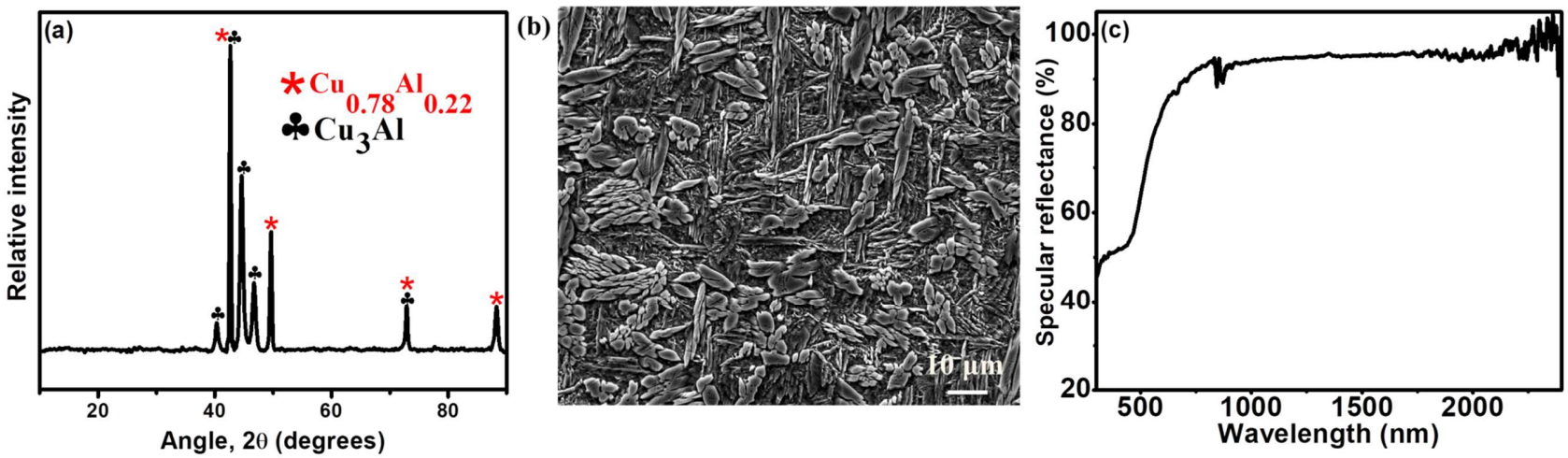

Fig. 1. Cu-21.2 atomic % Al alloy ingot (a) XRD pattern (b) Microstructure of polished surface and (c) Specular reflectance.

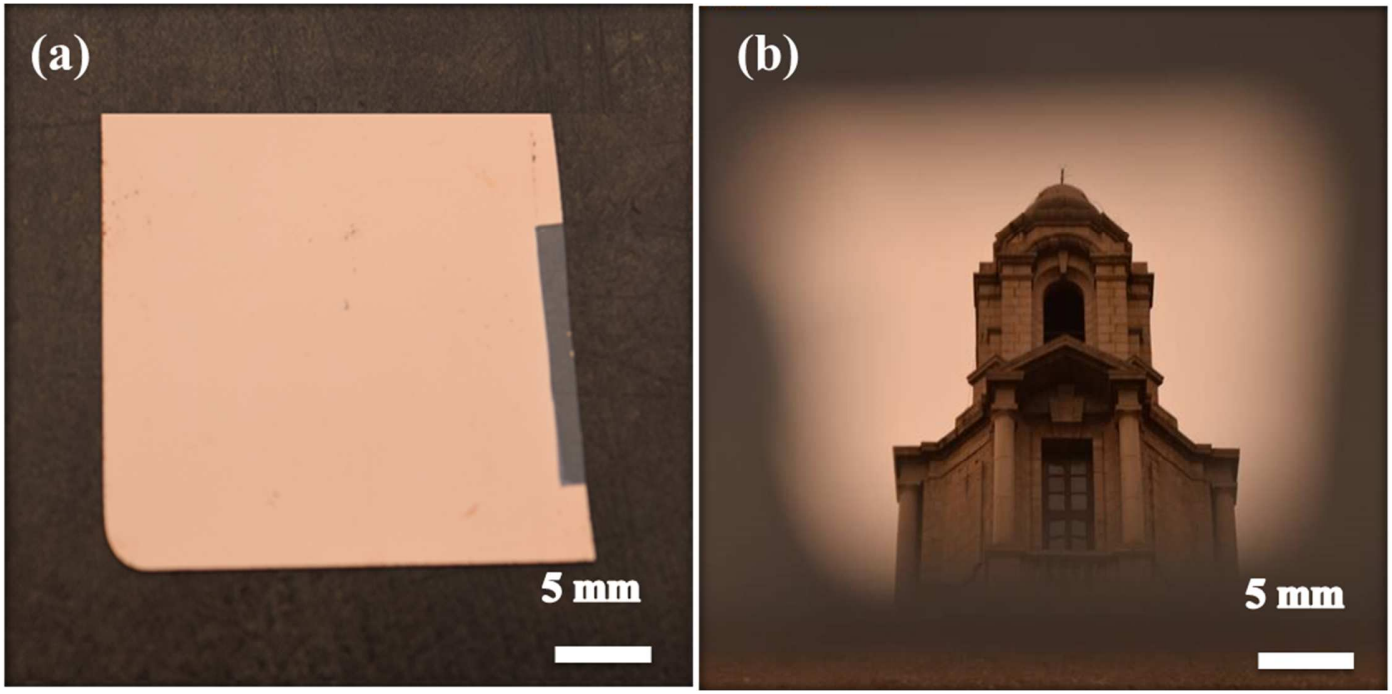

Fig. 2. Photographs of (a) as-deposited Cu-Al thin film on flexible glass and (b) showing clear reflection of tower building of IISc, Bangalore, imaged using Cu-Al thin film.

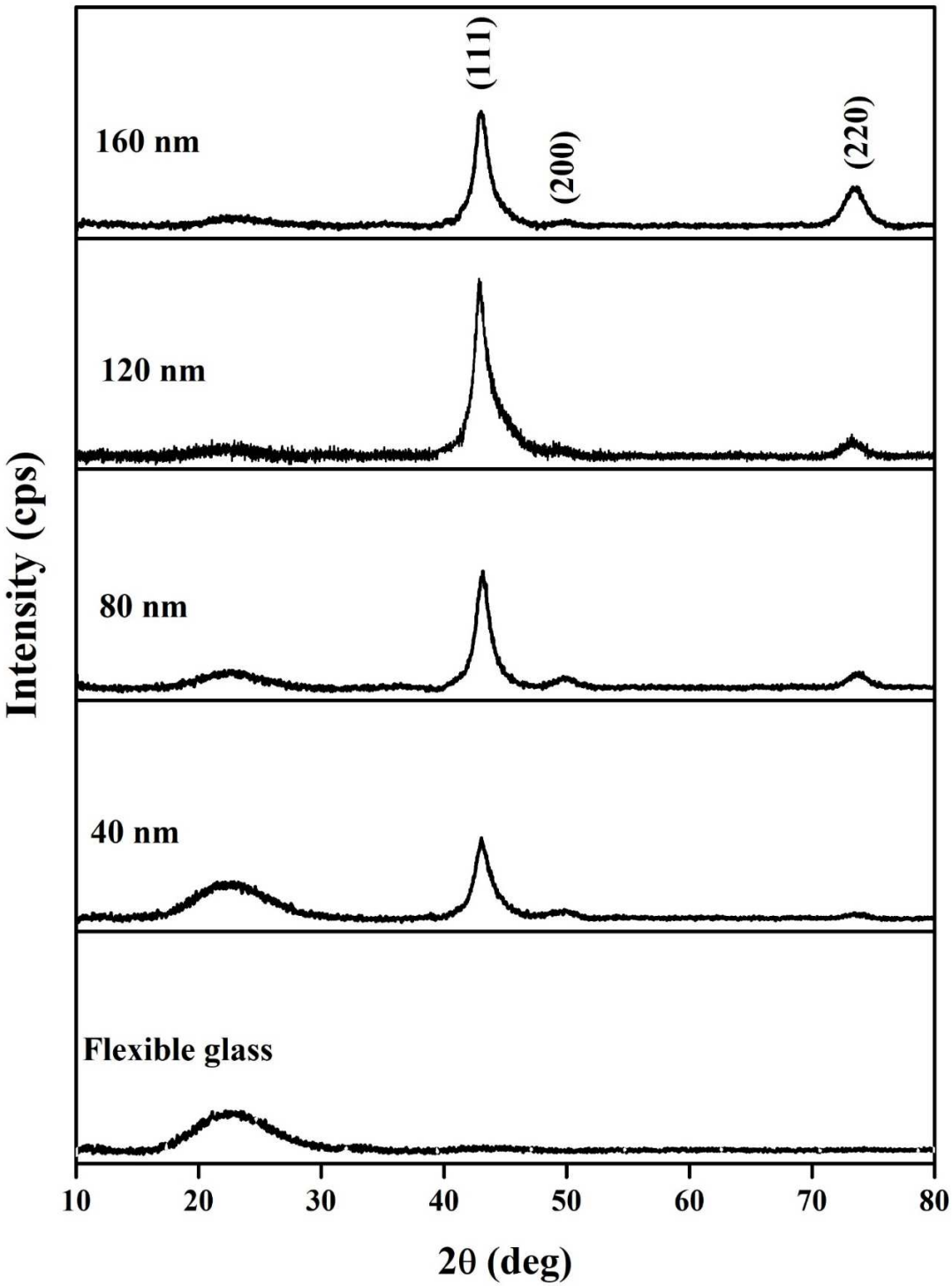

Fig. 3. Glancing angle XRD patterns of the Cu-Al films indicating the presence of $Cu_{0.78}Al_{0.22}$ with varying thickness on flexible glass substrates.

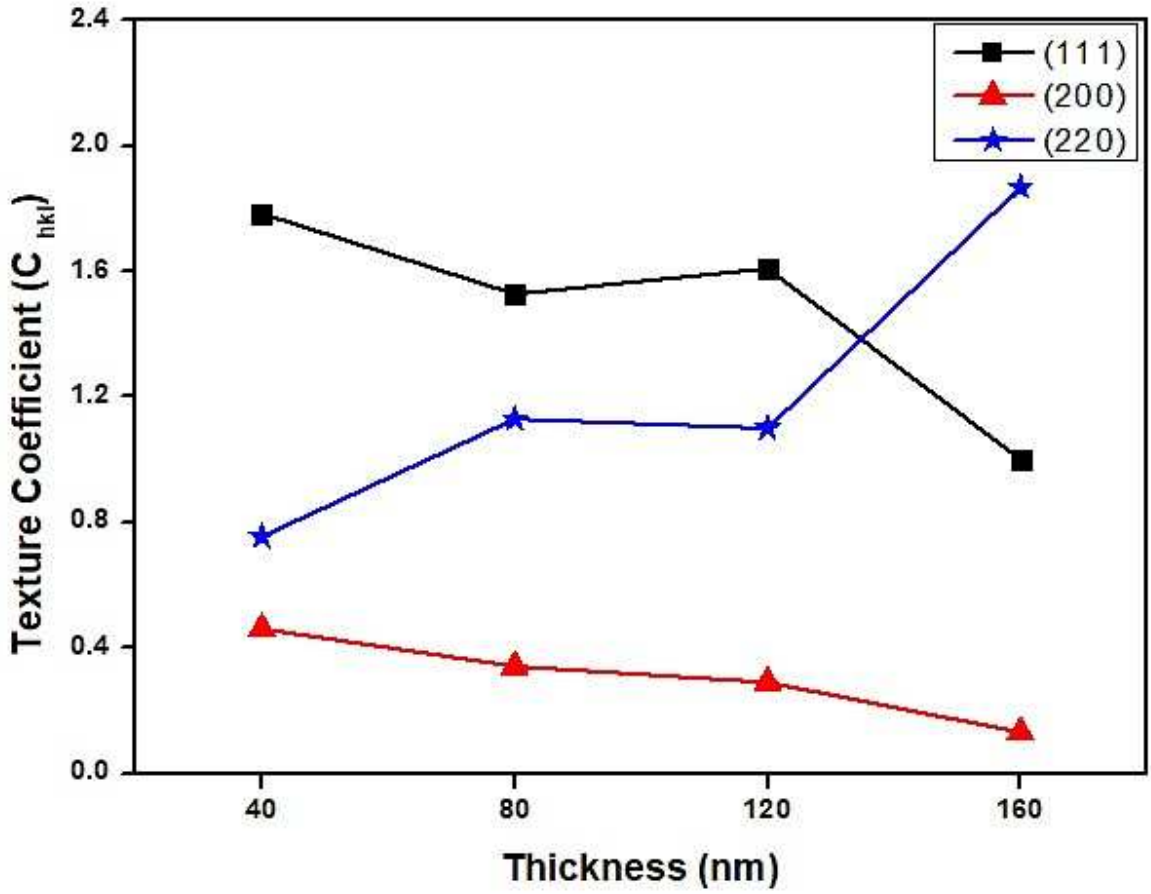

Fig. 4. Texture coefficient (TC) as a function of film thickness.

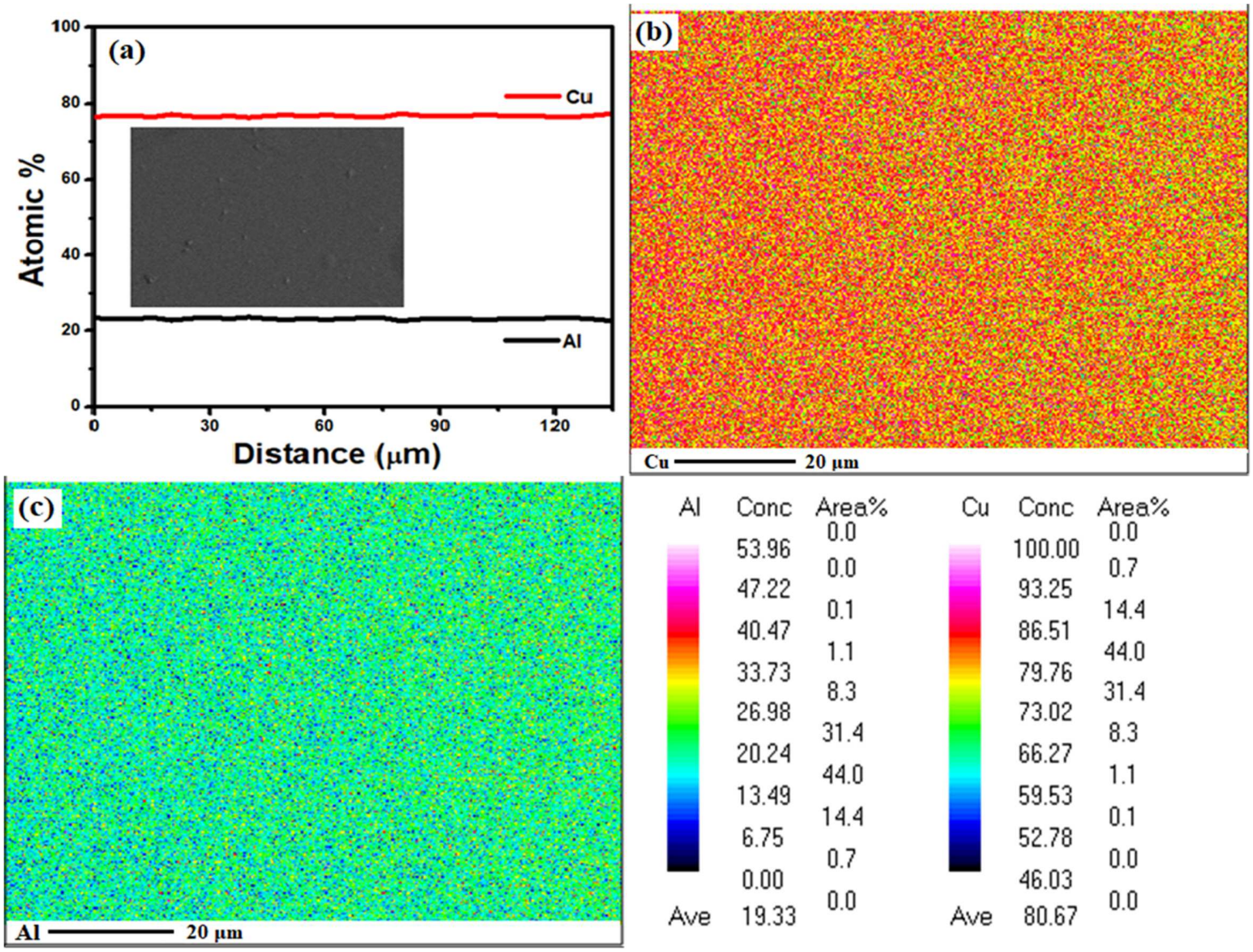

Fig. 5. (a) Compositional line scan (WDS) (b) Compositional mapping (WDS) of Cu and (c) Al of as-deposited 160 nm Cu-Al film on flex glass substrate

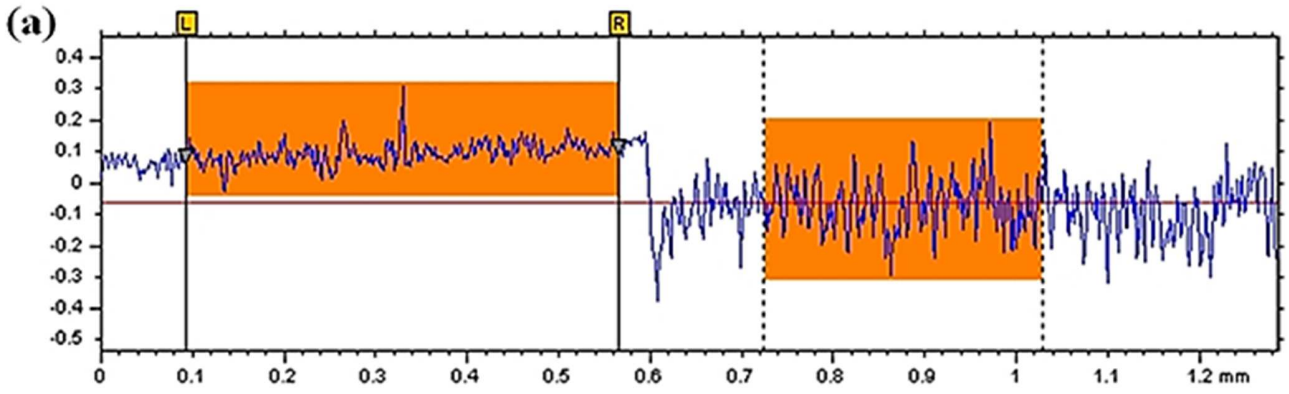

Maximum height	373.3 nm
Mean height	163.9 nm
Width	473.5 mm

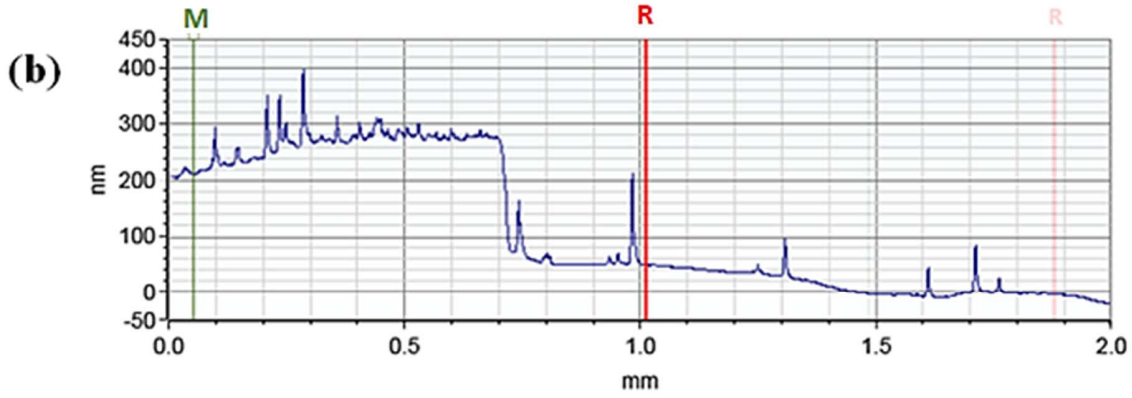

Label	Position (mm)	Height (nm)
R	1.01	51.7
M	0.05	211.8
Δ	-0.96	160.1

Fig. 6. (a) Optical profilometer and (b) Dektak profilometer measurements showing the thickness of the 160 nm thin film on flex glass substrate.

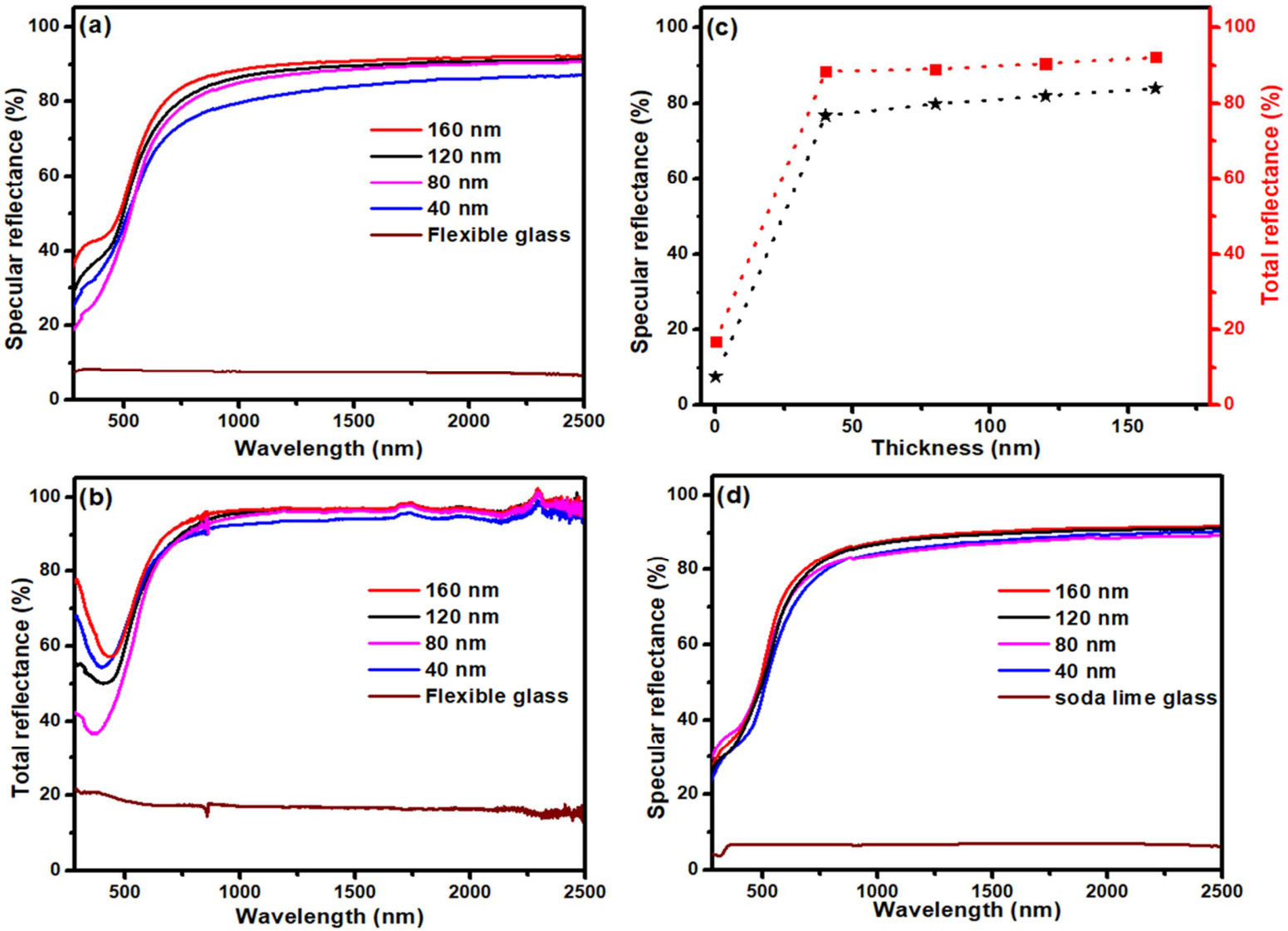

Fig. 7. (a) Specular reflectance and (b) total reflectance of the Cu-Al film on flexible glass with variation in wavelength of incident light. (c) The variation of specular reflectance and total reflectance with film thickness. (d) Specular reflectance of the Cu-Al film on soda lime glass as a function of wavelength of incident light.

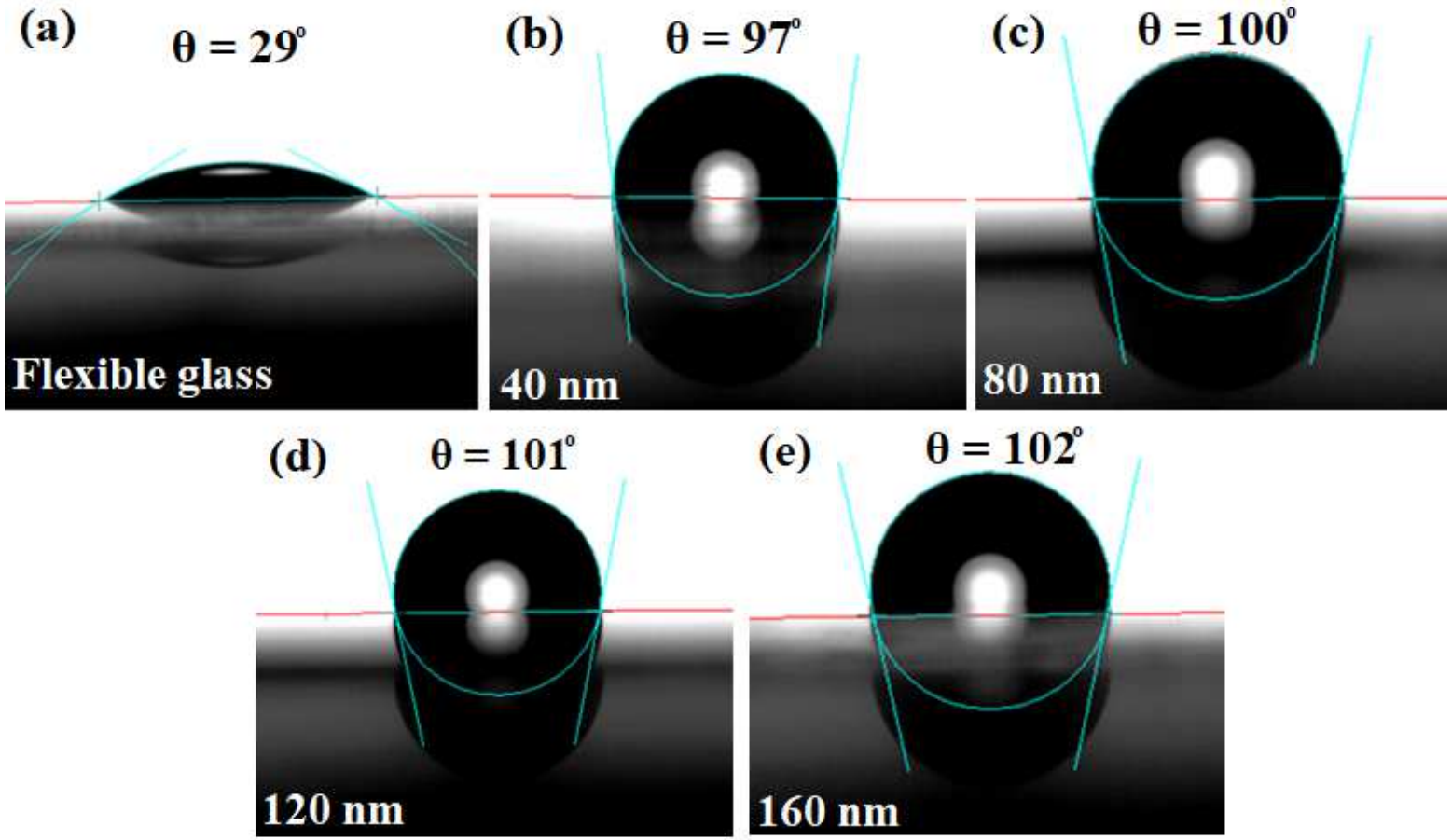

Fig. 8. Macroscopic image of water droplet shape on flexible glass and Cu-Al film with different thickness. Insignificant variation in contact angle observed and the magnitude of contact angles indicate hydrophobic nature.

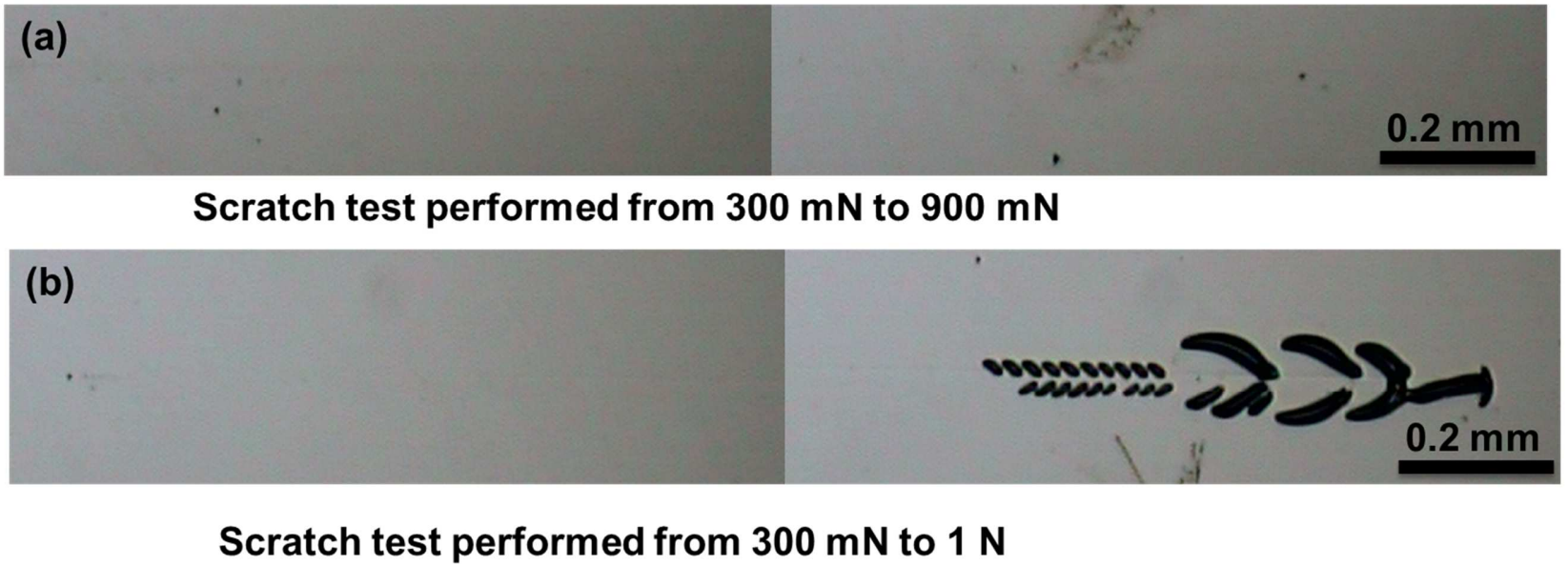

Fig. 9. Scratch test performed on Cu-Al film, indicating (a) no scratch till 900 mN and (b) occurrence of clear scratch beyond 900 mN.

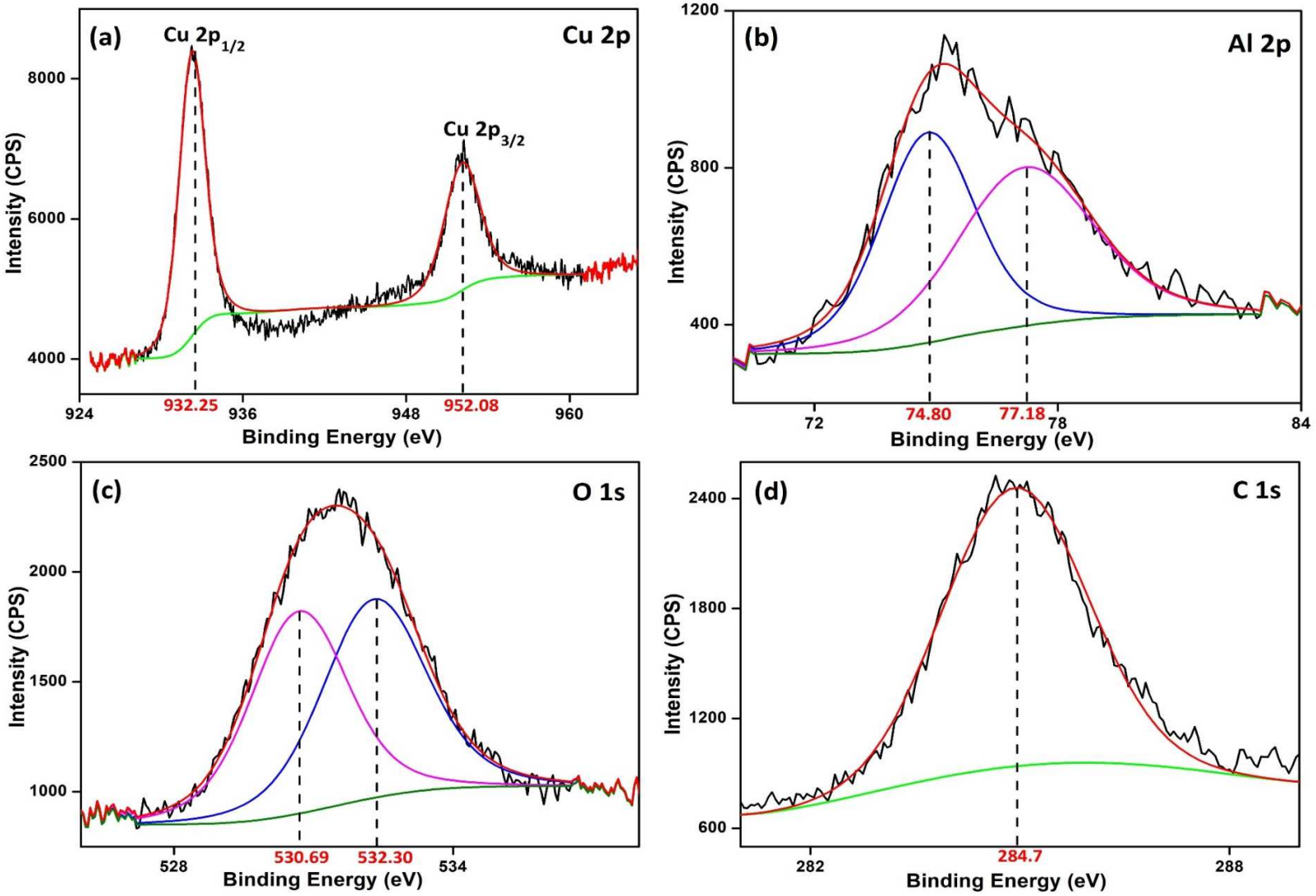

Fig. 10. XPS spectra recorded with Cu-Al bulk material (a) Cu 2p peaks (b) Al 2p peak (c) O 1s peak and (d) C1s reference peak

Table 1

Details of the work done to fabricate Cu-Al thin film on flex glass substrates by thermal evaporation.

Expected thickness (nm)	Thickness (nm) dektak	Thickness (nm) profilometer	Flex glass			Specular Reflectance (soda lime glass) %	Contact angle in degrees	Roughness parameter (nm)	
			Specular Reflectance %	Solar-weighted specular reflectance %	Total Reflectance %			R_a	R_q
160	160.1 ± 3.3	163.9 ± 5.8	83.9 ± 0.2	76.1	92.1 ± 0.6	82.8 ± 0.3	102.1 ± 0.7	7.1 ± 1.7	8.9 ± 2.3
120	119.9 ± 3.1	121.4 ± 3.9	81.9 ± 0.3	73.4	90.4 ± 0.5	81.9 ± 0.4	101.2 ± 1.3	6.6 ± 2.1	8.0 ± 1.7
80	80.2 ± 2.8	80.5 ± 1.3	79.8 ± 0.3	70.2	88.4 ± 0.7	80.4 ± 0.2	100.5 ± 0.4	6.9 ± 1.2	10.1 ± 2.1
40	41.2 ± 2.5	40.4± 2.7	76.7 ± 0.4	67.8	89.0 ± 0.6	79.9 ± 0.3	97.2 ± 1.7	7.3 ± 3.7	9.8 ± 3.2
Flex glass	-	-	7.5 ± 0.4	7.8	16.9 ± 0.8	6.7 ± 0.7	29.2 ± 2.3	6.4 ± 1.1	7.5 ± 1.8